# Spectroscopic study of pressure-polymerized phases of $C_{60}$

V. A. Davydov, L. S. Kashevarova, and A. V. Rakhmanina
*Institute of High Pressure Physics of the RAS, 142 092 Troitsk, Moscow Region, Russian Federation*

V. M. Senyavin
*Department of Chemistry, Moscow State University, Moscow 119 899, Russian Federation*

R. Céolin and H. Szwarc
*Laboratoire de Chimie Physique des Matériaux Amorphes, Université Paris XI, 91405 Orsay, France*

H. Allouchi and V. Agafonov
*Laboratoire de Chimie Physique, Faculté de Pharmacie de l'Université de Tours, 31 av. Monge, 37200 Tours, France*
(Received 2 November 1999; revised manuscript received 4 February 2000)

Comparative studies of the infrared (IR) and Raman spectra of the orthorhombic, tetragonal, and rhombohedral pressure-polymerized phases of $C_{60}$ as well as the pressure-dimerized state have been performed at ambient conditions. The tentative assignment of the vibrational spectra of different phases has shown that they could be perfectly described by the molecular symmetry of the $C_{60}$ polymers which are the structure-forming elements of crystalline polymerized phases. This allowed one to consider the IR and Raman spectra of the crystalline polymerized phases as characteristic of those of the appropriate one- and two-dimensional $C_{60}$ polymers and to use them for molecular fractional analysis of polymerization products.

## I. INTRODUCTION

The aim of this work was to carry out a comparative study of the vibrational spectra of all known crystalline polymerized phases (CPP's) obtained by pressure-temperature treatment of fullerite $C_{60}$.

The orthorhombic (*O*), tetragonal (*T*), and rhombohedral (*R*) CPP's, formed as a result of the $(2+2)$ cycloaddition reaction of $C_{60}$,[1] were identified in the works of Refs. 2 and 3. In doing so, Nuñez-Regueiro *et al.*[2] suggested structural models of these phases as molecular packing of the linear one-dimensional and two (tetragonal and trigonal) types of two-dimensional (2D) polymers of $C_{60}$ that we arbitrarily call the *O*, *T*, and *R* polymers. The principal validity of the suggested structural models of the CPP's was supported by numerous theoretical and experimental investigations.[4–19] However, at the same time these investigations have shown that initial data on identification and individual properties of CPP's require reexamination.

Until now it has been clear that the main reasons for discrepancies in the individual CPP properties determined by different authors are some difficulties in the synthesis of the pure CPP. That is why, despite the separate in-depth[8,12] and survey[11,15] spectroscopic investigations, the complete systematic study of the IR and Raman spectra of all the CPP's have not yet been carried out.

Our attention was therefore directed in particular to the synthesis of the single-phased samples of CPP's that were believed to correspond mainly to the structural models of optimal molecular packing of the *O*, *T*, and *R* polymers.[20–22] Successful synthesis of practically pure samples of the different CPP's allowed us to carry out the investigation of their individual infrared and Raman spectra in comparison with those of the initial monomeric fcc phase of $C_{60}$ and the high-pressure state composed mainly from the dumbbell-shaped $(C_{60})_2$ dimer[23–27] and to fulfill the tentative assignment of the main vibrational modes of the CPP's. The results obtained show that the IR and Raman spectra of the CPP's can be considered practically as the characteristic spectra of the *O*, *T*, and *R* polymers of $C_{60}$ and used for the molecular fractional analysis of the products of fullerene polymerization.

## II. EXPERIMENT

The CPP's were produced as a result of high-pressure high-temperature treatment (HPHTT) of fullerite $C_{60}$ in ''piston-cylinder''- and ''toroid''-type high-pressure devices. High-pure (99.98%), twice-sublimed small-crystalline fullerite $C_{60}$ supplied by Term USA was taken as a starting material. It was checked spectroscopically on the residual solvent contamination[28] which was found to reduce greatly the thermal stability of the sample. The initial powder was stored in in vacuum-sealed ampoules and was opened just prior to use. This procedure largely prevents the intercalation of oxygen in the bulk of material which could react with $C_{60}$ at high temperature.[29]

The *p*, *T* parameters and times of HPHTT chosen for synthesis of high-pressure phases were equal to 1.2 GPa, 573 K, 20 000 s; 2.2 GPa, 873 K, 2000 s; 6.0 GPa, 873 K, 2000 s; and 1.5 GPa, 423 K, 1000 s for the *O*, *T*, *R* ones and the dimerized state (DS), respectively. The appropriate *p*, *T* paths of HPHTT are shown in Fig. 1. The samples of high-pressure phases were conserved at ambient conditions by quenching them down to room temperature under pressure. Other details of HPHTT experiments have been described earlier.[13,30] It should be noted that we did not find the conditions of pure dimeric phase synthesis.[26,31] Because of this,

 

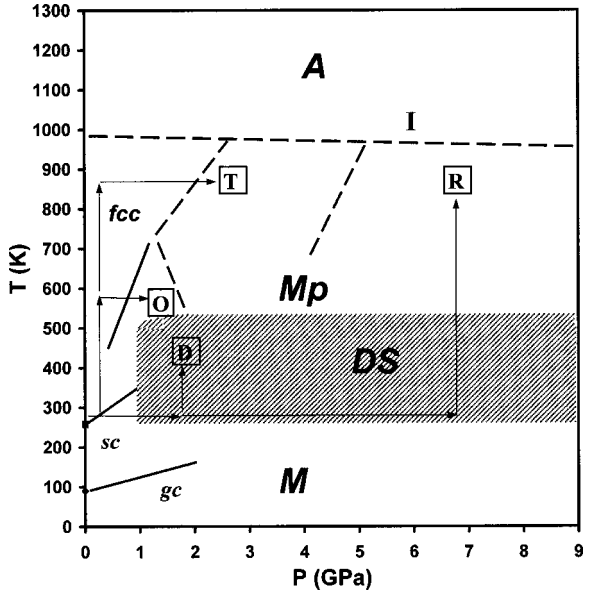


FIG. 1. Tentative *p, T* diagram of $C_{60}$. The arrows show *p, T* paths used for the synthesis of the *O*, *T*, and *R* phases at points *O*, *T*, and *R*; a state containing 80% of $(C_{60})_2$ was prepared at point *D*. The state enriched in $(C_{60})_2$ (dimerized state, DS) occupy a black zone. *Mp* corresponds to the range of the *O*, *T*, and *R* phases separated by dotted lines. *SC* is the $Pa3$ phase, *gc* is a glass phase. *A* represents the existence range of atomic carbon resulting from the destruction of the $C_{60}$ molecules.

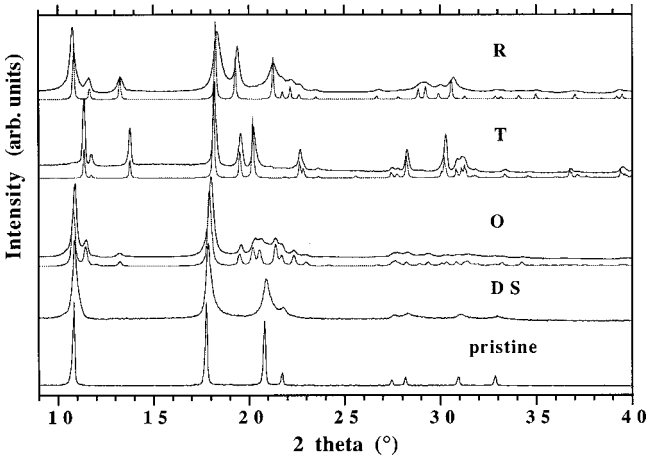


FIG. 2. XRD patterns for the pristine $C_{60}$, dimerized state (DS) and the *O*, *T*, and *R* phases (black: experimental, and dotted line: calculated).

the DS studied in this work was presented by the samples with the $(C_{60})_2$ content of about 80 mole %.

The initial checking of the quality of the CPP samples was made by the x-ray-diffraction (XRD) method. The highest-quality samples of the CPP were taken for the subsequent spectroscopic and microscopic investigations. The x-ray-diffraction experiments were carried out by means of an INEL CPS 120 position-sensitive detector using Cu$K\alpha_1$ radiation. Powdered samples were put into Lindemann glass capillaries of 0.5 mm in diameter which were rotated around the $\Theta$ axis during the experiments.

The IR transmission spectra of the samples pelletted in KBr were recorded on a Specord M80 (Karl Zeiss) spectrophotometer. The Raman spectra were investigated with a Brucker FT Raman RTS100 spectrometer and a Dilor *XY* spectrometer using Nd:YAG and $Ar^+/Kr^+$ lasers as excitation sources with wavelengths of 1064, 568.2, and 514.5 nm. All measurements were taken in a backscattering geometry. To avoid noticeable damage of samples during the experiments, the values of the power densities in the visible range were maintained at 0.2–1.5 W/cm$^2$.

Microscopic investigation of samples was carried out using DSM 982 Gemini, an electron-scanning microscope.

### III. RESULTS AND DISCUSSION

The experimental and calculated XRD patterns for the CPP are presented in Fig. 2 in comparison with the experimental patterns of the pristine $C_{60}$ and the DS. The structural characteristics of obtained CPP are given in Table I in comparison with the data of other authors.

It should be remarked that the quality of the experimental powdered XRD patterns does not allow us to determine unambiguously the space groups of the CPP. Therefore the structural model of these phases was adjusted on the basis of the energy calculations of *O*, *T*, and *R* polymer packings by the atom-atom potential method.[19–22] To date the theoretically predicted space groups for the *O* and *T* phases have already been confirmed experimentally.[18,32]

Comparison of experimental and calculated XRD patterns for the *O*, *T*, and *R* phases (Fig. 2) shows that there are practically no unindexed diffraction peaks in the experimental patterns. Thus the samples obtained are almost single phased and really present the molecular packing of the *O*, *T*, and *R* polymers of $C_{60}$.

Further experimental verification of this conclusion comes from the results of microscopic investigation. The micrographs of the sample slivers in Fig. 3 show the influence of the structure of the 1D and 2D polymers—the structure-forming elements of CPP—on the silver morphology. The details of the layer sequence parallel to the $(001)_T$ face and to the $(00.1)_R$ face can be seen in Figs. 3(b) and (c). The

TABLE I. Comparison of structural parameters of the all known polymerized phases of $C_{60}$.

| Phase | Space group | Cell parameters (Å) | | | $V$ Å$^3$, per mol. | Ref. |
|---|---|---|---|---|---|---|
| | | *a* | *b* | *c* | | |
| Pristine $C_{60}$ | $Fm\bar{3}m$ | 14.17 | | | 711 | This work |
| *O* | *Pmnn* | 9.098 | 9.831 | 14.72 | 658 | This work |
| | *Pmnn* | 9.14 | 9.90 | 14.66 | 663 | 18 |
| | *Immm* | 9.26 | 9.88 | 14.22 | 650 | 2 |
| | *Im3* | 9.23 | 10.00 | 14.32 | 661 | 10 |
| *T* | $P4_2/mmc$ | 9.097 | 9.097 | 15.02 | 622 | This work |
| | *Immm* | 9.09 | 9.09 | 14.95 | 618 | 2 |
| | $P4_2/mmc$ | 9.02 | 9.02 | 14.93 | 607 | 32 |
| *R* | $R\bar{3}m(60°)$ | 9.204 | | 24.61 | 602 | This work |
| | $R\bar{3}m$ | 9.19 | | 24.50 | 597 | 2 |
| | | 9.22 | | 24.6 | 603 | 3 |

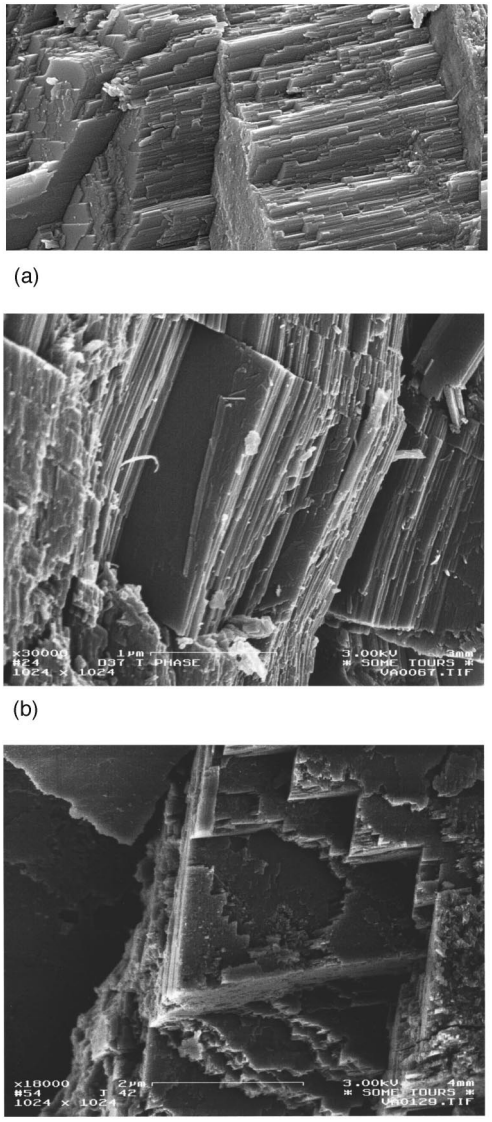


FIG. 3. Scanning electron microscope micrographs of the slivers of CPP samples: *O* phase (a), *T* phase (b), *R* phase (c).

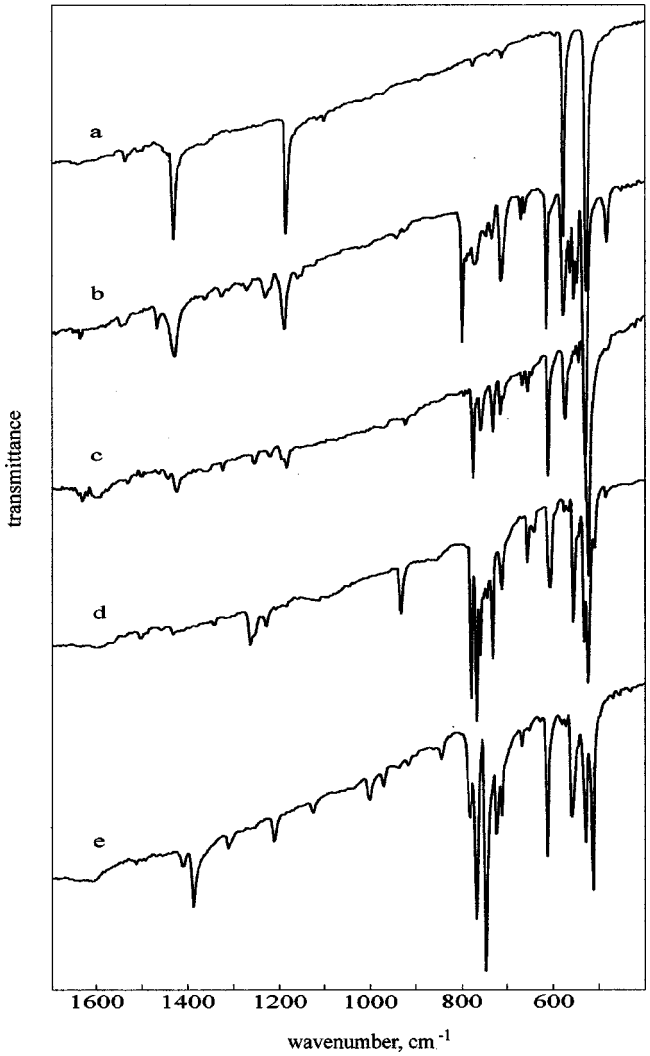


FIG. 4. IR spectra of the pristine $C_{60}$ (a), *O* (c), *T* (d), *R* (e) phases, and DS (b).

micrograph of the *O* phase [Fig. 3(a)] demonstrates in turn a fiberlike character of the structure.

The IR and Raman spectra of the pristine monomeric fcc phase of $C_{60}$, the DS, and the CPP are given in Figs. 4 and 5. Table II contains the assigned literature set of $C_{60}$ frequencies[33] as well as our IR and Raman data on pristine fullerene, the DS, and the *O*, *T*, and *R* phases of $C_{60}$. The Raman frequencies of the fcc phase, the DS, and the *O* phase are those from the spectra obtained under Nd:YAG laser excitation [Figs. 5(a)–(c)]; the frequencies of the *O*, *T*, and *R* phases are collected from $Kr^+$ line excited spectra [Figs. 5(d)–(f)]. The tentative assignment of CPP modes as derived from definite parent vibrations follows from their position in Table II. Note also that some weak features, e.g., near 850 $cm^{-1}$, remained unassigned.

The isolated $C_{60}$ molecule possesses $I_h$ symmetry, its 174 vibrations being distributed between 46 distinct modes according to irreducible representation:[34,35]

$$\Gamma_v = 2A_g + 3F_{1g} + 4F_{2g} + 6G_g + 8H_g + A_u + 4F_{1u} + 5F_{2u} + 6G_u + 7H_u .$$

From these, because of selection rules, only four modes of $F_{1u}$ symmetry are IR active and ten modes of $A_g$ and $H_g$ symmetry are allowed in Raman spectra; the remaining 32 modes are silent. At present, all vibrations are reliably assigned as a result of numerous experimental and theoretical investigations (for more details, see, e.g., Ref. 35). This work follows the exhaustive experimental interpretation of the $C_{60}$ spectra made by Martin *et al.*[33]

In the spectra of the crystalline monomeric phases of $C_{60}$, some additional features are observed caused by the lower site symmetry of the molecules in the lattice, the symmetry of the cage position being $T_h$ in the fcc phase and $S_6$ in the low-temperature simple cubic phase.[34–37] In thick layers and reflectivity measurements, the combination modes could also be observed.[33,35,38] Generally, these crystal-field effects dominate over the isotopic substitution[39–42] and both of them cause much weaker spectral bands than those corresponding to the IR- and Raman-active modes of the $C_{60}$ molecule.

The situation is changed drastically by the formation of $C_{60}$ polymers. The formation of intercage covalent bonds

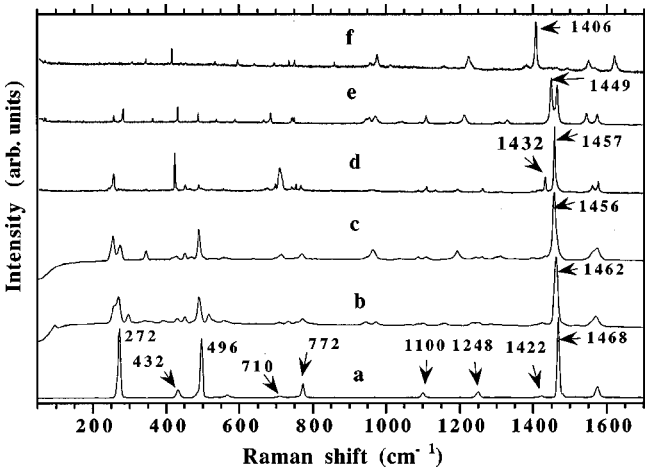


FIG. 5. Raman spectra of the pristine $C_{60}$ (a), DS (b), and *O* phase (c), excited by a 1064-nm line; those of the *O* (d), *T* (e), and *R* (f) phases, excited by a 568.2-nm line.

vigorously reduces the molecular symmetry and gives rise to pronounced changes of the vibrational spectra.[3,43–46] Assuming the regularity and sufficient extension of the polymers, they could be treated spectroscopically as monomeric links. Hence one should expect either $D_{2h}$ molecular symmetry in the *O* and *T* phases or $D_{3d}$ symmetry in the *R* one. Such a lowering of symmetry should activate the silent modes of $C_{60}$ and result in appropriate splitting of all of the degenerate modes, and some additional bands should be observed corresponding to the vibrations of bonding fragments. Thus the dramatic symmetry reduction becomes the decisive factor that determines the structure of the vibrational spectra (Figs. 4 and 5). The role of the crystal-field effect and natural isotopic $^{13}C$ substitution could be evaluated, e.g., by the violation of the mutual exclusion rule in the spectra of all polymeric systems being center symmetric because all polymeric systems should retain the inversion center.

The tentative assignment of the spectra was generally fulfilled according to the group-theoretical predictions of mode activity within the chosen point group, and the splitting of the allowed and silent modes of $C_{60}$ under a definite reduction of symmetry. The correlation between the $I_h$, $D_{2h}$, and $D_{3d}$ symmetry point groups could be established readily using the tables of characters. Such tables have been given earlier, but several misprints in Table I published in Ref. 12 need some comments. While the omission of the $B_{3u}$ component in the reduction of the $H_u$ mode under the $D_{2h}$ perturbation did not affect the declared ''$0\rightarrow3$'' splitting, the misprints in the part of the table devoted to the $D_{3d}$ symmetry led to an improper number of the expected IR and Raman bands. In Table III the correct correlation is therefore given.

As can be seen, on the symmetry reduction to the $D_{3d}$ point group, the $G_g$ and $H_g$ modes should split in the Raman spectrum into two and three components respectively, while the triply degenerate *F* modes could be activated as singlets only, because of the inactivity of the $A_{2g}$ species. All of the odd icosahedral modes should split into doublets in the IR spectrum, the only forbidden mode being the $A_{1u}$ species. As the result, 45 lines could be observed in the Raman spectrum of the $C_{60}$ cage distorted by the $D_{3d}$ symmetry ($16A_{1g}+29E_g$), and 44 bands ($15A_{2u}+29E_u$) in IR. In the case of the $D_{2h}$ symmetry, the numbers of IR- and Raman-active modes are correspondingly equal to 66 ($B_{1u}$, $B_{2u}$, $B_{3u}$) and 87 ($A_g$, $B_{1g}$, $B_{2g}$, $B_{3g}$), as has already been noted.[8,12]

The $(C_{60})_2$ molecule belongs also to the $D_{2h}$ point group but, in contrast to the cases of the *O* and *T* polymers, where the inversion center could be placed in the center of a cage, in the dimer molecule it is situated in the center of a four-member cycle. Thus the symmetry of the cage is $C_{2v}$. The loss of the inversion center by the cage should not only remove the degeneracy but also activate all degenerate icosahedral modes both in the Raman and IR spectra. In the $(C_{60})_2$ molecule such ''low-symmetry'' motions of the cages would combine to yield both odd and even collective vibrations (with respect to the molecular center of inversion), in accordance with the $D_{2h}$ overall symmetry.

These symmetry species should, of course, obey the mutual exclusion rule intrinsic to the point group, but for the purposes of tentative assignment it is important to mention that the derivatives of all degenerate icosahedral modes could be observed in both the Raman and the IR spectra of the dimer. As for the nondegenerate modes of the cage, each of them gives one even and one odd vibration of the $(C_{60})_2$ molecule: $2A_g(C_{60})\rightarrow A_g+B_{1u}[(C_{60})_2]$; $2A_u(C_{60})\rightarrow A_u+B_{1g}[(C_{60})_2]$. Hence the $A_g$ derivatives might be observed both in the Raman and the IR spectra, while the $A_u$ derivatives is active only in the Raman scattering. As a result, 134 ($B_{1u}$, $B_{2u}$, $B_{3u}$) and 177 ($A_g$, $B_{1g}$, $B_{2g}$, $B_{3g}$) modes are expected correspondingly in the IR and Raman spectra of the $(C_{60})_2$ molecule, taking into account also interball vibrations.

The group-theoretical analysis thus predicts more than 300 modes in the $(C_{60})_2$ molecule, more than 150 vibrations of the distorted $C_{60}$ cage in the *O* and *T* polymers, and almost 100 modes in the link of the *R* polymer distributed between the IR and Raman spectra with the slight numerical superiority of the latter. The real IR and Raman spectra both consist only of some tens of well-distinguished bands with frequencies which do not coincide, apart from a few exceptions (Figs. 4 and 5 and Table II). This suggests that no additional symmetry reduction (caused by effects other than chemical bonding) play an essential role. The reason for there being so few bands in the experimental spectra of polymeric species, in comparison with the predicted number, lies presumably in the insufficient intensity of some bands. Sometimes the occasional degeneracy of frequencies takes place in the spectra of the dimer. Nevertheless, the majority of parent modes are observed and assigned in the spectra of polymers of $C_{60}$.

In the IR spectrum of the dimer, the four $F_{1u}$-derived bands are readily seen, their weighed center being within a 3-$cm^{-1}$ interval from the parent modes. The relative intensities of $F_{1u}(2-4)$ modes drop. The bands at 526 and 574 $cm^{-1}$ possess asymmetric contours; the width of the 1426-$cm^{-1}$ band rises to 20 $cm^{-1}$, and the $F_{1u}(3)$ parent mode splits into a doublet of 1184/1189 $cm^{-1}$ with a low-frequency shoulder. The splitting of the parent modes in the chained polymer is more pronounced: the shoulder near 530 $cm^{-1}$ at $F_{1u}(1)$ band is resolved, the width of the band at 576 $cm^{-1}$ is twice of that of the $F_{1u}(2)$ mode of $C_{60}$ or its analog in the dimer molecule; the bands appear at 1195 and

TABLE II. The vibrational modes of the pristine, DS, and polymerized phases of $C_{60}$ with their assignment.

| | fcc $C_{60}$ | | DS | | *O* | | *T* | | *R* | |
|---|---|---|---|---|---|---|---|---|---|---|
| [33] | IR | *R* | IR | *R* | IR | *R* | IR | *R* | IR | *R* |
| 1600 $H_u(7)$ | | | | | | | | | | |
| 1596 $G_g(6)$ | | | | | | | | | | 1626 |
| | | | | | | | | | | 1620 |
| 1576 $H_g(8)$ | | 1574 | | 1570 | | 1572 | | 1573 | | 1567 |
| 1567 $H_g(8)$ | | | | 1556 | | 1560 | | | | 1550 |
| 1544 $F_{2g}(4)$ | 1540 | | | | | | | 1544 | | 1538 |
| 1526 $G_u(6)$ | | | | 1518 | | | | | | |
| 1484 $F_{1g}(3)$ | | | | | | | | 1465 | | 1493 |
| 1479 $F_{1g}(3)$ | | | | | | | | | | |
| 1470 $A_g(2)$ | | 1468 | 1464 | 1462 | | 1457 | | 1449 | | 1406 |
| 1433 $F_{1u}(4)$ | | | | | 1446 | | | | 1405 | |
| 1429 $F_{1u}(4)$ | 1428 | | 1426 | | 1426 | | | | 1383 | |
| 1425 $H_g(7)$ | | 1422 | | 1424 | | 1432 | | | | 1381 |
| 1418 $H_g(7)$ | | | | 1403 | | 1396 | | | | |
| 1345 $G_g(5)$ | | | | 1348 | | 1350 | | 1328 | | 1354 |
| | | | | | | | | | | 1333 |
| 1330 $G_g(4)$ | | | | | | 1310 | | 1308 | | 1315 |
| | | | | | | 1297 | | 1296 | | 1292 |
| 1313 $F_{2u}(5)$ | 1312 | | 1321 | | 1326 | | 1346 | | 1306 | |
| | | | | | 1319 | | 1342 | | | |
| 1290 $G_u(5)$ | 1295 | | | 1283 | | | | | | |
| 1252 $H_g(6)$ | | 1248 | | 1250 | | 1260 | | 1259 | | 1229 |
| | | | | 1233 | | 1243 | | | | 1222 |
| 1242 $H_u(6)$ | 1240 | | 1246 | | 1260 | | 1263 | | | |
| | | | | | 1255 | | 1254 | | | |
| | | | | | 1246 | | | | | |
| 1222 $H_u(5)$ | 1218 | | 1230 | | 1228 | | 1228 | | | |
| | | | 1226 | | 1222 | | | | | |
| | | | 1219 | | 1214 | | | | | |
| 1214 $F_{2g}(3)$ | | | | | | | | 1211 | | 1208 |
| 1199 $G_g(3)$ | | | | | | 1192 | | 1176 | | 1186 |
| | | | | 1159 | | | | | | 1158 |
| 1183 $F_{1u}(3)$ | 1184 | | 1189 | | 1195 | | | | 1206 | |
| | | | 1184 | | 1183 | | | | 1121 | |
| | | | 1180 | | | | | | | |
| 1122 $A_u$ | 1120 | | | | | | | | | |
| 1102 $H_g(5)$ | 1100 | 1100 | | 1102 | | 1109 | | 1109 | | 1077 |
| | | | | 1088 | | 1086 | | 1092 | | |
| 1080 $G_u(4)$ | | | | 1059 | | | | | | |
| 1038 $F_{2u}(4)$ | 1040 | | | | | 1040 | | 1044 | | 1012 |
| | | | | | | | | 1034 | | |
| 973 $F_{1g}(2)$ | | | | 972 | | 965 | | 970 | | 977 |
| 961 $G_g(2)$ | 963 | | 940 | 943 | | 945 | | 955 | | 956 |
| | | | | | | | | 945 | | |
| 828 $H_u(4)$ | 828 | | 920 | | 924 | | 932 | | 998 | |
| | | | | | | | 898 | | 966 | |
| | | | | | | | 882 | | | |
| | | | | | | 853 | | 864 | 838 | 858 |
| 797 $F_{2u}(3)$ | | | 796 | 801 | 778 | | 780 | | 778 | |
| | | | 785 | 792 | | | 768 | | | |
| 778 $H_g(4)$ | 776 | 772 | 770 | 772 | | 770 | | 748 | | 768 |

TABLE II. (*Continued*).

| | fcc $C_{60}$ | | DS | | *O* | | *T* | | *R* | |
|---|---|---|---|---|---|---|---|---|---|---|
| [33] | IR | *R* | IR | *R* | IR | *R* | IR | *R* | IR | *R* |
| 775 $H_g(4)$ | | | 767 | 755 | | 753 | | 743 | | 749 |
| | | | | | 742 | | 735 | | 733 | |
| 764 $F_{2g}(2)$ | 765 | | 762 | | | | | | | |
| 753 $G_u(3)$ | | | 755 | | 759 | | 765 | | 764 | |
| | | | 747 | | | | 762 | | | |
| | | | 742 | | | | | | | |
| 739 $G_u(2)$ | 739 | | 737 | 733 | 738 | | 747 | | 743 | |
| | | | 732 | | 730 | | 741 | | | |
| | | | 728 | | 728 | | 730 | | | |
| 712 $F_{2u}(2)$ | 712 | | 711 | | 716 | | 716 | | 718 | |
| | | | 706 | | 711 | | 711 | | 709 | |
| | | | | | 708 | | | | | |
| 709 $H_g(3)$ | | 710 | | 708 | | 714 | | 713 | | 709 |
| | | | | | | 697 | | 685 | | 695 |
| | | | | | | 676 | | 667 | | |
| 668 $H_u(3)$ | 668 | | 668 | | 668 | 668 | 654 | | 663 | |
| 664 $H_u(3)$ | | | 660 | | 656 | | 646 | | 646 | |
| | | | | | 649 | | 642 | | | |
| 578 $H_u(2)$ | | | 613 | | 612 | 614 | 605 | | 608 | |
| | | | | | | 596 | | | | |
| 577 $F_{1u}(2)$ | 576 | | 574 | 576 | 576 | 577 | 565 | | 555 | |
| | | | | | | | 555 | | 550 | |
| | | | | | | | 546 | | | |
| 568 $F_{1g}(1)$ | | 567 | 561 | | 562 | 566 | | 588 | | 595 |
| | | | 550 | 556 | 554 | 556 | | 566 | | 559 |
| 541 $F_{2g}(1)$ | | | 546 | | 543 | | | 538 | | 533 |
| 526 $F_{1u}(1)$ | 526 | | 526 | 528 | 530 | | 532 | | 524 | 523 |
| | | | | 515 | 526 | | 522 | | 509 | |
| | | | | | | | 510 | | | |
| 495 $A_g(1)$ | | 496 | 486 | 490 | | 488 | | 487 | | 487 |
| 485 $G_g(1)$ | | | 478 | | | 471 | | | | 470 |
| 431 $H_g(2)$ | | 432 | 450 | 450 | | 452 | | 453 | | 453 |
| | | | 441 | 430 | | 427 | | 432 | | 440 |
| | | | 428 | | | | | | | 415 |
| 402 $G_u(1)$ | | | | 402 | | | | | | |
| | | | | 392 | | | | | | |
| 353 $F_{2u}(1)$ | | | | 365 | | | | 363 | | |
| 342 $H_u(1)$ | | | | 342 | 338 | 346 | | | | 344 |
| 272 Hg(1) | | 272 | | 295 | | 274 | | 282 | | 306 |
| | | | | 269 | | 256 | | 279 | | 273 |
| | | | | 256 | | | | 258 | | 243 |
| | | | | 95 | | | | | | |

1446 $cm^{-1}$ as a result of the splitting of the $F_{1u}(3-4)$ modes. In the *T* and *R* polymers, the $F_{1u}(1)$ mode demonstrates the expected behavior, splitting into a triplet with components at 510, 522, 532, $cm^{-1}$ and into a doublet of 509/524 $cm^{-1}$, respectively. The $F_{1u}(2)$ mode in the *R* phase also splits into two moderate lines of equal intensity (550 and 555 $cm^{-1}$), while in the *T* phase one strong line at 555 $cm^{-1}$ and two very weak features at 546 and 565 $cm^{-1}$ are observed. No marked bands were found in the region of the $F_{1u}(3-4)$ modes for the tetragonal structure. A sharp moderate line at 1383 $cm^{-1}$ and a weak band at 1405 $cm^{-1}$ are the candidates for the $F_{1u}(4)$ derivatives in the spectra of the *R* phase; the $F_{1u}(3)$ mode splits into 1121 and 1206-$cm^{-1}$ bands.

As was mentioned in the earliest IR study of polymeric states of $C_{60}$,[3] the maximum of activity from silent modes is gained in a 700–800 $cm^{-1}$ spectral range. This is hardly surprising, because in this narrow interval the parent molecule possesses four modes of odd symmetry at 712 $[F_{2u}(2)]$, 739 $[G_u(2)]$, 753 $[G_u(3)]$, and 797 $[F_{2u}(3)]$ $cm^{-1}$ that should be activated.[33]

The most remarkable features in the IR spectrum of the

TABLE III. Correlation table of symmetry groups $I_h$, $D_{2h}$, and $D_{3d}$.

| $I_h$ | $D_{2h}$ | Splitting | $D_{3d}$ | Splitting |
|---|---|---|---|---|
| $A_g$ | $A_g$ | $1\rightarrow1$ | $A_{1g}$ | $1\rightarrow1$ |
| $F_{1g}$ | $B_{1g}+B_{2g}+B_{3g}$ | $0\rightarrow3$ | $A_{2g}+E_g$ | $0\rightarrow1$ |
| $F_{2g}$ | $B_{1g}+B_{2g}+B_{3g}$ | $0\rightarrow3$ | $A_{2g}+E_g$ | $0\rightarrow1$ |
| $G_g$ | $A_g+B_{1g}+B_{2g}+B_{3g}$ | $0\rightarrow4$ | $A_{1g}+A_{2g}+E_g$ | $0\rightarrow2$ |
| $H_g$ | $2A_g+B_{1g}+B_{2g}+B_{3g}$ | $1\rightarrow5$ | $A_{1g}+2E_g$ | $1\rightarrow3$ |
| $A_u$ | $A_u$ | $0\rightarrow0$ | $A_{1u}$ | $0\rightarrow0$ |
| $F_{1u}$ | $B_{1u}+B_{2u}+B_{3u}$ | $1\rightarrow3$ | $A_{2u}+E_u$ | $1\rightarrow2$ |
| $F_{2u}$ | $B_{1u}+B_{2u}+B_{3u}$ | $0\rightarrow3$ | $A_{2u}+E_u$ | $0\rightarrow2$ |
| $G_u$ | $A_u+B_{1u}+B_{2u}+B_{3u}$ | $0\rightarrow3$ | $A_{1u}+A_{2u}+E_u$ | $0\rightarrow2$ |
| $H_u$ | $2A_u+B_{1u}+B_{2u}+B_{3u}$ | $0\rightarrow3$ | $A_{1u}+2E_u$ | $0\rightarrow2$ |

dimer in this region are the strong band at 796 $cm^{-1}$ and the doublet at 711/706 $cm^{-1}$. They are readily assigned as derived from $F_{2u}$ (3 and 2) modes, respectively. The band at 785 $cm^{-1}$ might formally be regarded as the other component of the former, but its nature is thought to be quite different and will be discussed below. The weak triplet of 728/732/737 $cm^{-1}$ is assigned to the $G_u(2)$ derivative; the bands at 747 (with low-frequency shoulder) and at 755 $cm^{-1}$ (very weak) originate from the $G_u(3)$ mode.

There are two additional features to be assigned: the moderate band at 770 $cm^{-1}$ (with a shoulder at 767 $cm^{-1}$) and the sharp line at 762 $cm^{-1}$. The reason for their appearance is an activation of icosahedral even modes in the IR spectrum of the $(C_{60})_2$ molecule, namely those of the $H_g(4)$ and the $F_{2g}(2)$, respectively. The validation of this symmetry-predicted phenomenon was also found in the other spectral regions.

The IR spectra of the *O*, *T*, and *R* polymers in this region are simpler, as was expected. The $F_{2u}(2)$ mode in the polymeric species splits into doublets with close wave numbers (711–716 $cm^{-1}$ in the *O* and *T* phases and 709–718 $cm^{-1}$ in the *R*) but quite different relative intensities. In the *O* polymer, the band at 711 $cm^{-1}$ has a pronounced shoulder that may be the third component of the splitting. The $G_u(2)$ mode transforms into triplets of 728/730/738 and of 730/741/747 $cm^{-1}$ in the spectra of chained and tetragonal polymers, respectively, and into the most intense band at 743 $cm^{-1}$ in the spectrum of the *R* phase. Strong narrow lines at 759 (*O*), 762 (*T*), and 764 (*R*) $cm^{-1}$ originate from the $G_u(3)$ mode of $C_{60}$. The $F_{2u}(3)$ cage mode softens to 778 (*O, R*) and 780 (*T*) $cm^{-1}$. The band in the *O* polymer is fairly broad and possibly includes another component of splitting. In the spectra of the *T* phase this component is included in the broad band at 768 $cm^{-1}$, the rest of the band being composed from the component of the $G_u(3)$ mode.

In a 600–700 $cm^{-1}$ spectral region, the features characteristic of all pressure-polymerized forms of $C_{60}$ are observed. The strong band at 613 (*D*), 612 (*O*), 605 (*T*), 608 (*R*) $cm^{-1}$ is a clear indication of the modification of the cage, the only reasonable explanation of its origin being a significant ($\sim$ 30 $cm^{-1}$) blue shift of the $H_u(2)$ parent mode. Slightly higher, the group of the $H_u(3)$ derivatives is observed to be strictly in accordance with symmetry predictions: the bands at 660 (broad) and 668 $cm^{-1}$ in the dimer, well-resolved triplets at 649/656/668 and 642/646/654 $cm^{-1}$ for the *O* and *T* polymers, and a doublet at 646/663 $cm^{-1}$ in the *R* phase, respectively.

In the region between the $F_{1u}(1)$ and the $F_{1u}(2)$ modes, the moderate bands at 546, 550, and 561 $cm^{-1}$ were observed in the spectra of the dimer and weak features at 543, 554, and 562 $cm^{-1}$ were found for the chained polymer. The emergence of the lines could not be linked to the $F_{1u}$ modes, because they are already split in the spectra of these samples. Even leaving aside the asymmetric contours and shoulders on the $F_{1u}(1,2)$ derivatives, the distance between the observed features is too large to originate from that splitting, especially in comparison with the cases of the *T* and *R* phases. Note also that there are no analogs for these bands in the spectra of 2D polymers. The bands were therefore assigned as originating from the $F_{1g}(1)$ and $F_{2g}(1)$ modes of $C_{60}$. While the appearance of these bands in the spectrum of the dimer is not surprising, their observation in the chained structure should be explained. In our opinion, the emergence of symmetry-forbidden modes in the sample of the *O* polymer suggests either the contribution of even-member oligomers or another sort of transitional state, e.g., branched structures. The presence of the same species is believed also to cause the band at 785 $cm^{-1}$, best distinguished in the spectra of the dimerized state. The band was assigned to the $F_{2u}(3)$ derived vibration of this product because: (i) it is absent in the spectra of any pure polymeric phase as well as in the spectrum of synthetic $(C_{60})_2$;[24] (ii) its relative intensity rises in the spectra of mixtures; (iii) the position of the band is intermediate between its analogs (796 and 778 $cm^{-1}$) in the dimer and the *O* polymer.

In a 400–500-$cm^{-1}$ region, only the IR spectrum of the dimer demonstrates distinguishable features: a moderate band at 478 $cm^{-1}$ with a shoulder at 486 $cm^{-1}$, originating from the $G_g(1)$ and $A_g(1)$ modes, and several weak bands at 450, 441, and 428 $cm^{-1}$ arising from the $H_g(2)$ mode. Below 400 $cm^{-1}$, because of the interference of atmospheric water absorption, the results are less reliable, but the derivatives of the $G_u(1)$ and $F_{2u}(1)$ modes are seen in all spectra near 380 and 360 $cm^{-1}$, respectively. The broad feature at 338 $cm^{-1}$ in the spectra of the *O* polymer arises from the $H_u(1)$ mode.

In the range of the so-called ''fingerprints region'' (800–1000 $cm^{-1}$), several bands appear characteristic of each polymer, as regards both their wave numbers and their intensity. In the spectra of the dimer, two very weak features are observed near 920 and 940 $cm^{-1}$; a weak band at 924 $cm^{-1}$ belongs to the chained polymer. The *T* phase demonstrates the band at 932 $cm^{-1}$ (the most intense of all the phase in this region) and weak bands at 882 and 898 $cm^{-1}$. Two weak bands at 966 and 998 $cm^{-1}$ are found in the spectra of the *R* polymer. The nearest parent modes with odd symmetry are the $H_u(4)$ mode at 828 $cm^{-1}$ and the $F_{2u}(4)$ mode at 1038 $cm^{-1}$,[33] both being equally distant from the bands under discussion. However, the systematic blue shift of the bands suggests that their common origin is positioned at a lower frequency. We therefore assign these bands as originating from the $H_u(4)$ mode.

Above 1000 $cm^{-1}$, except for the $F_{1u}$-derived modes, few weak and moderate bands are observed. The triplets at 1219/1226/1230 and 1214/1222/1228 $cm^{-1}$ and a broad band at

1228 $cm^{-1}$ in the spectra of the dimer and the *O* and *T* polymers, respectively, originate from the $H_u(5)$ mode; the very weak band of the dimer at 1246 $cm^{-1}$ and the multiplets at 1246/1255/1260 $cm^{-1}$ (*O*) and 1254/1263 $cm^{-1}$ (*T*) originate from the $H_u(6)$ mode. The $F_{2u}(5)$ derivatives are observed (in the same sequence) at 1321, 1319/1326, and 1342/1346 $cm^{-1}$ and at 1306 $cm^{-1}$ for the *R* phase. The band at 1464 $cm^{-1}$ in the spectrum of the dimer was assigned to the $A_g(2)$ derivative, being, in the absence of other candidates, one of the clearest indications of the loss of the inversion center by the $C_{60}$ moiety.

When comparing the Raman spectra of the polymerized states of $C_{60}$, one should take into account the preresonant conditions of excitation in visible and near-IR spectral ranges. For pristine fullerene, the phenomenon leads to drastic changes in the relative intensities of allowed vibrational bands when going from green (514.5 nm) to IR (1064 nm) laser lines, and to the observation of the silent $F_{1g}(1)$ mode at 567 $cm^{-1}$ in the latter case. The process of polymerization affects the electronic structure of the material, produces defects in the solid, and hence additionally changes the conditions for possible resonance. For the substances which have been discussed up to now, the electron absorption spectra of the synthetic dimer[23,24] and the *R* polymer[6,47,48] were reported. They demonstrated only the structureless tails of absorption in the vicinity of exciting lines used in the present study, as well as for pristine material. Nevertheless, our experiments obtained some indirect evidence, such as the relative intensities of the bands and the magnitude and shape of the luminescent background, which suggested that electronic effects are involved. It was found that the Raman spectra of the dimer and the chained polymer of $C_{60}$ were most informative upon near-IR excitation when using the Fourier transform (FT) registration technique. The spectra of the *T* and *R* polymers had better quality when excited by green or yellow lines of the $Ar^+/Kr^+$ laser. We therefore do not discuss the systematic transformation of the spectra upon polymerization, but describe only the shifts and splitting of the icosahedral modes that were observed under optimal conditions of registration.

In the FT Raman spectrum of the pressure-dimerized samples [Figs. 5(a)–(c)], the redshifts of the $A_g$(1 and 2) modes of $C_{60}$ are correspondingly equal to 6 and 8 $cm^{-1}$. The degeneracy of $H_g$ modes is partially removed: the $H_g(1)$ mode splits, at least, into triplet, whereas most of the other $H_g$ modes split into doublet. From the derivatives of other even modes, the most prominent are those of the $G_g(2)$ and $F_{1g}(2)$ modes at 943 and 972 $cm^{-1}$, the rest being present as shoulders or as very weak features. Odd parent modes are represented by $G_u$ derivatives at 392/402, 733, 1059, and 1283 $cm^{-1}$, as well as those of $H_u(1)$, $F_{2u}(1)$, and $F_{1u}(1)$ modes at 342, 365, and 515/528 $cm^{-1}$. A new band appearing at 95 $cm^{-1}$ can be assigned to the totally symmetric interball vibration. This value is in reasonable agreement with the best theoretical prediction.[49] It should also be mentioned that the spectrum obtained coincides strictly with that of synthetic $(C_{60})_2$,[25] and, in contrast to IR, does not contain any additional details.

In the spectrum of the chained polymer, the $A_g$ (1, 2) parent modes soften to 8 and 12 $cm^{-1}$. The magnitude of the splitting of the $H_g$ modes rises. The derivatives of odd icosahedral modes disappear in agreement with symmetry predictions. The bands originating from even modes gain in intensity, presumably the $G_g$(1,3,4) and $F_{1g}(2)$ derivatives at 471, 1192, 1310, and 965 $cm^{-1}$, respectively. At the same time, the elevated background makes it difficult to examine the low-frequency region.

The Raman spectra of the DS and the *O* phase under green (514.5 nm) line excitation are much less informative. In both cases the rise of activity was observed in the vicinity of the $H_g$ modes and the derivatives of the $F_{1g}(2)$ and $G_g(2)$ modes appear below 1000 $cm^{-1}$. The spectrum of the *O* polymer excited by the yellow $Kr^+$ line (568.2 nm) contains more features [Fig. 5(d)]. In comparison with near-IR excitation, a remarkable redistribution of spectral intensity takes place, not only between the derivatives of different modes but also within the components of each split icosahedral vibration. Among the clearest examples is the transformation of the $H_g$ modes. The derivative of the $H_g(1)$ mode is observed as a band at 257 $cm^{-1}$ with low-frequency shoulders and a very weak feature at 271 $cm^{-1}$, instead of a near-IR-excited doublet at 256/274 $cm^{-1}$; the $H_g(2, 3)$ modes (which were weak broad bands at 427 and 714 $cm^{-1}$) rise upon yellow excitation to strong bands at 425 and 710 $cm^{-1}$, respectively, being the second and third in intensity throughout the whole spectrum. The $H_g(4)$ mode splits into a triplet at 742/753/767 $cm^{-1}$, while the $H_g(8)$ mode splits into a doublet 1560/1575 $cm^{-1}$. The intensity of the $A_g(1)$ band falls dramatically.

In contrast to previous cases, the Raman spectra of the *T* and *R* phases under green excitation possess a satisfactory signal-to-noise ratio. The spectra of the *T* polymer have been described elsewhere:[30] the preferential activation of a single component for most of the degenerate modes allowed one to assign a one-to-one correspondence between each observed band and a definite parent vibration. Besides the $A_g$ and $H_g$ derivatives, the bands originating from all of the $F_{1g}$, $F_{2g}$, and most of the $G_g$ modes were detected. The $A_g(2)$ and $H_g(3)$ modes softened to 1449 and 667/685 $cm^{-1}$ respectively, while the $F_{1g}(1)$ derivative was blue shifted to a 563/587-$cm^{-1}$ doublet. The usage of a yellow exciting line led to a more uniform distribution of spectral intensity [Fig. 5(e)]. Along with the $H_g(2)$ band (which remained the most intense in the low-frequency range), the components of the $H_g$(1,3,4,) modes and the $A_g(1)$ derivative gained significant intensity. Dramatic intensity redistribution took place below 1000 $cm^{-1}$ resulting in the splitting of the $G_g(2)$ mode into a 948/956-$cm^{-1}$ doublet; a considerable enhancement of the $G_g(4, 5)$ and $F_{2g}(4)$ lines was observed. There was little difference between the Raman spectra of the *R* polymer when excited by either green or yellow laser lines. The redshift of the $A_g(2)$ mode enriches its maximum, value: the corresponding line was detected at 1406 $cm^{-1}$. The shifts of the weighed center of other modes were not so large, while the value of splitting rose to some tens of $cm^{-1}$. In the high-frequency range the derivative of the $G_g(6)$ mode is observed as a moderate band at 1620 $cm^{-1}$ with a shoulder at 1626 $cm^{-1}$ [Fig. 5(f)].

The results obtained in the present study thus attest that the main features of the vibrational spectra of polymerized states with defined molecular constitution can be really perfectly described by molecular symmetry.[12] That is, the vibra-

tional spectra of the *O*, *T*, and *R* phases can be practically considered as identical to those of the *O*, *T*, and *R* polymers. The determination of the individual vibrational spectra of CPP permits us to make some remarks with reference to the spectral characteristics of different high-pressure polymerized states of $C_{60}$ which were published previously.

Regarding the IR spectra, the overall agreement of our results was observed only with data on the *R* phase. Better accordance was found with the spectra of Kamaras *et al.*,[12] Kozlov *et al.*,[47] and Iwasa *et al.*,[48] which were free from a broad feature at 1100 $cm^{-1}$ caused by oxygen contamination present in other works.[3,11,15,16] Only a few bands of *T* polymer and no spectral features of *O* phase can be found in the survey IR spectra of Rao and co-workers.[11,15]

Raman spectroscopy revealed that the spectra of the *O* and *R* phases presented in Refs. 3, 11, and 15 are not those of the individual *O* and *R* phases. This is most conspicuous by the presence of the bands at 1447 and 1464 $cm^{-1}$, which are associated with the *T* phase in the Raman spectrum of the assumed *R* phase. At the same time, although our Raman spectra of the *O* phase are in qualitative agreement with those of the pressure-polymerized $C_{60}$ obtained at 1.1 GPa and 573 K,[6,8,14] a more careful analysis of the spectra shows that the material obtained presents a mixture of chained polymers and $(C_{60})_2$ dimers. In our opinion, it is this fact that explains the observed two-component structure of the $A_g(2)$ derivative, but not the Davydov splitting as was suggested.[8]

The interpretation of the spectra carried out in the present work can be compared only with the consideration of some regions of the IR spectra of the *R* phase[12] and with the details of the splitting of $H_g$ modes in the Raman spectra of the sample in Ref. 8. In the first case, agreement is achieved in the assignment of the derivatives of the $F_{1u}(1-4)$ and, possibly, $F_{2u}(2)$ and $H_u(3)$ modes. Commenting on the interpretation of the Raman spectra in Ref. 8, it could be mentioned that the band near 340 $cm^{-1}$ is observed as in the *O* polymer, as in the *R* phase, and as in dimerized $C_{60}$. Hence it could not be a ''very good fingerprint''[8] and a characteristic of the formation of the *O* phase.

## IV. CONCLUSION

To conclude, the complete vibrational characterization of practically pure CPP of $C_{60}$ was fulfilled. The application of group-theoretical analysis enabled us to propose a tentative assignment of the IR and Raman spectra and to follow the transformation of most of the icosahedral modes upon reduction of symmetry in the polymerized states of $C_{60}$. At the same time, the values of the shifts and the magnitude of the splitting of the parent modes in polymeric systems are not considered in the symmetry approach, since these are determined by the changes in geometry and in the intramolecular interactions taking place upon the linkage of the balls. Some ambiguity therefore always exists when ascribing the bands in the spectra of polymers to a definite vibration of the parent molecule. A more complete understanding might be achieved by appropriate calculations of the vibrational properties of appropriate systems, and in part by the normal coordinate analysis that is now in progress.

## ACKNOWLEDGMENTS

The present research has been supported by INTAS, Grant No. 93-2133, and by the Russian Fund for Fundamental Research, Grant No. 97-03-33584a. The authors thank G. Sagon (LADIR-CNRS, Thiais, France) and P. Y. Sizaret (Service de la Microscopie Electronique de l'Université de Tours) for technical assistance.

[1] A. M. Rao, P. Zhou, K. A. Wang, G. T. Hager, J. M. Holden, Y. Wang, W. T. Lee, X.-X. Be, P. C. Eklund, D. S. Cornett, M. A. Duncan, and I. J. Amster, Science **259**, 955 (1993).

[2] M. Nuñez-Regueiro, L. Marques, J-L. Hodeau, O. Berthoux, and M. Perroux, Phys. Rev. Lett. **74**, 278 (1995).

[3] Y. Iwasa, T. Arima, R. M. Fleming, T. Siegrist, O. Zhou, R. C. Haddon, L. J. Rothberg, K. B. Lyons, H. L. Carter, Jr., A. F. Hebard, R. Tycko, G. Dabbagh, J. J. Krajevski, G. A. Thomas, and T. Yagi, Science **264**, 1570 (1994).

[4] C. H. Xu and G. E. Scuseria, Phys. Rev. Lett. **74**, 274 (1995).

[5] G. Oszlanyi and L. Forro, Solid State Commun. **93**, 265 (1995).

[6] P. A. Persson, U. Edlund, P. Jacobsson, D. Jonels, A. Soldatov, and B. Sundqvist, Chem. Phys. Lett. **258**, 540 (1996).

[7] T. Gozé, F. Rachdi, L. Hajji, M. Nuñez-Regueiro, L. Marques, J.-L. Hodeau, and M. Mehring, Phys. Rev. B **54**, 3676 (1996).

[8] J. Winter, H. Kuzmany, A. Soldatov, P.-A. Persson, P. Jacobsson, and B. Sundqvist, Phys. Rev. B **54**, 17 486 (1996).

[9] L. Marques, J.-L. Hodeau, M. Nuñez-Regueiro, and M. Perroux, Phys. Rev. B **54**, R12 633 (1996).

[10] C. S. Sundar, P. Ch. Sahu, V. S. Sastry, G. V. Rao, V. Sridharan, M. Premila, A. Bharathi, Y. Hariharan, and T. S. Radhakrishnan, Phys. Rev. B **53**, 8180 (1996).

[11] A. M. Rao, P. C. Eklund, J.-L. Hodeau, L. Marques, and M. Nuñez-Regueiro, Phys. Rev. B **55**, 4766 (1997).

[12] K. Kamaras, Y. Iwasa, and L. Forro, Phys. Rev. B **55**, 10 999 (1997).

[13] V. A. Davydov, L. S. Kashevarova, A. V. Rakhmanina, V. Agafonov, R. Ceolin, and H. Szwarc, Carbon **35**, 735 (1997).

[14] T. Wägberg, P. A. Persson, B. Sundqvist, and P. Jacobsson, Appl. Phys. A: Mater. Sci. Process. **A64**, 223 (1997).

[15] A. M. Rao, P. C. Eklund, U. D. Venkateswaran, J. Ticker, M. A. Dunkan, G. M. Bendele, P. W. Stephens, J.-L. Hodeau, L. Marques, M. Nuñez-Regueiro, I. O. Bashkin, E. G. Ponyatovsky, and A. P. Moravsky, Appl. Phys. A: Mater. Sci. Process. **A64**, 231 (1997).

[16] M. E. Kozlov, M. Tokumoto, and K. Yakushi, Appl. Phys. A: Mater. Sci. Process. **A64**, 241 (1997).

[17] V. Agafonov, V. A. Davydov, L. S. Kashevarova, A. V. Rakhmanina, A. Kahn-Harari, P. Dubois, R. Céolin, and H. Szwarc, Chem. Phys. Lett. **267**, 193 (1997).

[18] R. Moret, P. Launois, P.-A. Persson, and B. Sundqvist, Europhys. Lett. **40**, 55 (1997).

[19] V. A. Davydov, L. S. Kashevarova, A. V. Rakhmanina, A. V. Dzyabchenko, V. Agafonov, P. Dubois, R. Céolin, and H. Szwarc, Pis'ma Zh. Eksp. Teor. Fiz. **66**, 110 (1997) [JETP Lett. **66**, 120 (1997)].

[20] V. A. Davydov, V. Agafonov, A. V. Dzyabchenko, R. Céolin, and H. Szwarc, J. Solid State Chem. **141**, 164 (1998).
[21] A. V. Dzyabchenko, V. Agafonov, and V. A. Davydov, Crystallogr. Rep. **44**, 13 (1999).
[22] A. V. Dzyabchenko, V. Agafonov, and V. A. Davydov, Crystallogr. Rep. **44**, 18 (1999).
[23] G. W. Wang, K. Komatsu, Y. Murata, and M. Shiro, Nature (London) **387**, 583 (1997).
[24] K. Komatsu, G. W. Wang, Y. Murata, T. Tanaka, K. Fujiwara, K. Yamamoto, and M. Saunders, J. Org. Chem. **63**, 9358 (1998).
[25] S. Lebedkin, A. Gromov, S. Giesa, R. Gleiter, B. Renker, H. Rietschel, and W. Krätschmer, Chem. Phys. Lett. **285**, 210 (1998).
[26] V. A. Davydov, L. S. Kashevarova, A. V. Rakhmanina, V. M. Senyavin, V. Agafonov, R. Céolin, and H. Szwarc, Pis'ma Zh. Eksp. Teor. Fiz. **68**, 881 (1998) [JETP Lett. **68**, 928 (1998)]
[27] V. A. Davydov, L. S. Kashevarova, A. V. Rakhmanina, V. Agafonov, H. Allouchi, R. Céolin, A. V. Dzyabchenko, V. M. Senyavin, H. Szwarc, T. Tanaka, and K. Komatsu, J. Phys. Chem. B **103**, 1800 (1999).
[28] V. M. Senyavin, A. A. Kurskaya, I. L. Odinets, M. V. Korobov, and R. S. Ruoff, in *Fullerenes Recent Advances in the Chemistry and Physics of Fullerenes and Related Materials*, edited by K. M. Kadish and R. S. Ruoff (ECS, Pennington, NJ, 1997), Vol. 5, p. 580.
[29] H. Werner, Th. Schedel-Niedrig, M. Wohlers, D. Herein, B. Herzog, R. Schlogl, M. Keil, A. M. Bradshaw, and J. Kirschner, J. Chem. Soc., Faraday Trans. **90**, 403 (1994).
[30] V. A. Davydov, L. S. Kashevarova, A. V. Rakhmanina, A. V. Dzyabchenko, V. Agafonov, H. Allouchi, R. Céolin, A. V. Dzyabchenko, V. M. Senyavin, and H. Szwarc, Phys. Rev. B **58**, 14 786 (1998).
[31] A. V. Dzyabchenko, V. Agafonov, and V. A. Davydov, J. Phys. Chem. A **103**, 2812 (1999).
[32] R. Moret, P. Launois, T. Wagberg, and B. Sundqvist (unpublished).
[33] M. C. Martin, X. Du, J. Kwon, and L. Mihaly, Phys. Rev. B **50**, 173 (1994).
[34] M. Matus and H. Kuzmany, Appl. Phys. A: Solids Surf. **A56**, 241 (1993).
[35] M. S. Dresselhaus, G. Dresselhaus, and P. C. Eklund, *Science of Fullerenes and Carbon Nanotubes* (Academic, New York, 1996).
[36] W. Kräschmer, L. D. Lamb, K. Fostiropoulos, and D. R. Hoffman, Nature (London) **347**, 345 (1990).
[37] P. H. M. van Loosdrecht, P. J. M. van Bentum, and G. Meijer, Chem. Phys. Lett. **205**, 191 (1993).
[38] P. Bowmar, W. Hayes, M. Kurmoo, P. A. Pattenden, M. A. Green, P. Day, and K. Kikuchi, J. Phys.: Condens. Matter **6**, 3161 (1994).
[39] D. E. Weeks, J. Chem. Phys. **96**, 7380 (1992).
[40] Z.-H. Dong, P. Zhou, J. M. Holden, P. C. Eklund, M. S. Dresselhaus, and G. Dresselhaus, Phys. Rev. B **48**, 2862 (1993).
[41] S. P. Love, D. Mc. Branch, M. I. Salkola, N. V. Coppa, J. M. Robinson, B. I. Swanson, and A. R. Bishop, Chem. Phys. Lett. **225**, 170 (1994).
[42] L. Akselrod, H. J. Byrne, S. Donovan, and S. Roth, Chem. Phys. **192**, 307 (1995).
[43] M. C. Martin, D. Koller, X. Du, P. W. Stephens, and L. Mihaly, Phys. Rev. B **49**, 10 818 (1994).
[44] D. Koller, M. C. Martin, and L. Mihaly, Mol. Cryst. Liq. Cryst. Sci. Technol., Sect. A **256**, 275 (1994).
[45] M. C. Martin, D. Koller, A. Rosenberg, C. Kendziora, and L. Mihaly, Phys. Rev. B **51**, 3210 (1995).
[46] K. Kamaras, D. B. Tanner, L. Forro, M. C. Martin, L. Mihaly, H. Klos, and B. Gotschy, J. Supercond. **8**, 621 (1995).
[47] M. E. Kozlov and K. Yakushi, J. Phys.: Condens. Matter **7**, L209 (1995).
[48] Y. Iwasa, T. Furudate, T. Fukawa, T. Ozaki, T. Mitani, T. Yagi, and T. Arima, Appl. Phys. A: Mater. Sci. Process. **A64**, 251 (1997).
[49] D. Porezag, M. R. Pederson, Th. Frauenheim, and Th. Kohler, Phys. Rev. B **52**, 14 963 (1995).